Published in final edited form as:
Cell Rep. 2014 June 26; 7(6): 1771–1778. doi:10.1016/j.celrep.2014.05.028.

Synaptic Control of Secretory Trafficking in Dendrites

Cyril Hanus[1,*], **Lisa Kochen**[1], **Susanne tom Dieck**[1], **Victor Racine**[2], **Jean-Baptiste Sibarita**[3], **Erin M. Schuman**[1], and **Michael D. Ehlers**[4,*]

[1]Max Planck Institute for Brain Research, Frankfurt 60438, Germany

[2]Institute of Molecular & Cell Biology, Agency for Science, Technology and Research, Singapore 138673, Singapore

[3]Interdisciplinary Institute for Neuroscience, Bordeaux 33077, France

[4]Neuroscience Research Unit, Pfizer Worldwide Research and Development, Cambridge, MA 02139, USA

Summary

Localized signaling in neuronal dendrites requires tight spatial control of membrane composition. Upon initial synthesis, nascent secretory cargo in dendrites exits the endoplasmic reticulum (ER) from local zones of ER complexity that are spatially coupled to post-ER compartments. Although newly synthesized membrane proteins can be processed locally, the mechanisms that control the spatial range of secretory cargo transport in dendritic segments are unknown. Here, we monitored the dynamics of nascent membrane proteins in dendritic post-ER compartments under regimes of low or increased neuronal activity. In response to activity blockade, post-ER carriers are highly mobile and are transported over long distances. Conversely, increasing synaptic activity dramatically restricts the spatial scale of post-ER trafficking along dendrites. This activity-induced confinement of secretory cargo requires site-specific phosphorylation of the kinesin motor KIF17 by Ca^{2+}/calmodulin-dependent protein kinases (CaMK). Thus, the length scales of early secretory trafficking in dendrites are tuned by activity-dependent regulation of microtubule-dependent transport.

Introduction

Local protein synthesis modifies the composition and functional properties of dendritic segments and associated synapses (Govindarajan et al., 2011; Sutton et al., 2006). mRNAs encoding neurotransmitter receptors and voltage-gated channels are among the cohort of dendritic mRNAs (Cajigas et al., 2012), supporting the notion that key mediators of dendritic excitability and neurotransmission are synthesized locally in dendrites. For

[*]Correspondence: cyril.hanus@brain.mpg.de (C.H.), michael.ehlers@pfizer.com (M.D.E.).

Author contributions

C.H. designed and performed the experiments, analyzed the results, and wrote the manuscript. L.K. designed and performed the experiments, analyzed the results, and edited the manuscript. S.t.D. cloned GS27 and edited the manuscript. V.R. and J.-B.S. provided Multidimensional Image Analysis (MIA). E.M.S. designed the experiments and edited the manuscript. M.D.E. designed the experiments and wrote the manuscript.

Europe PMC Funders Author Manuscripts

cytoplasmic proteins, local synthesis requires only mRNA, ribosomes, and soluble cofactors, and hence can occur as a point source of new polypeptides at the site of translation. In contrast, integral membrane proteins and secreted proteins require all of the machinery of the secretory pathway. Specifically, after synthesis in the endoplasmic reticulum (ER), membrane proteins progress through the ER-Golgi intermediate compartment (ERGIC), the Golgi apparatus (GA), and the *trans*-Golgi network (TGN), where they are modified before delivery to the plasma membrane. Although virtually all of the machinery for protein synthesis, ER import and export, and Golgi membranes have been detected in dendrites (Hanus and Ehlers, 2008), the route followed by nascent cargo after ER exit and the mechanisms that spatially direct post-ER transport in dendrites remain central unresolved issues in neuronal cell biology. Recent studies have shown that nascent cargo can be confined in microdomains of the dendritic ER specialized for ER export (Cui-Wang et al., 2012). Following ER exit, membrane cargo can be either transported over long distances in dendrites or trafficked locally (Horton and Ehlers, 2003). This choice is an essential determinant of cargo fate, yet there is little understanding of how post-ER transport is regulated to control secretory cargo destination.

Along with the machinery that controls membrane fission, docking, and fusion, molecular motors orchestrate cargo exchange between cellular compartments and are key effectors of membrane trafficking (Hirokawa et al., 2010; Kennedy and Ehlers, 2011; Südhof and Rothman, 2009). Motor-based transport is particularly important in neuronal axons and dendrites, whose development, maintenance, and plasticity require the transport of mRNAs, membrane proteins, and organelles up to hundreds of microns to meters from the soma. During intracellular transport, neurotransmitter receptors and ion channels associate with protein complexes that physically interact with specific molecular motors (Hirokawa et al., 2010), allowing tailored regulation of cytoskeleton-based transport. Several mechanisms that control motor-cargo interactions have been described. For example, local Ca^{2+}-dependent mechanisms regulate the association of myosin Vb with Rab11-FIP2 adaptor complexes on AMPA receptor-containing recycling endosomes (Wang et al., 2008), allowing local regulation of actin-based transport in dendritic spines. On the other hand, microtubule-based transport in dendrites is governed by dynein and kinesin motors whose action is important for synaptic function (Govindarajan et al., 2011; Hirokawa et al., 2010). Among the various kinesins, KIF5 and KIF17 are particularly important for long-range trafficking in neuronal processes. In contrast to KIF5, which is involved in the transport of a large cast of axonal and dendritic proteins (Hirokawa et al., 2010), far fewer cargos have been identified for KIF17. Those identified include kainate receptors (Kayadjanian et al., 2007), NMDA receptors (Setou et al., 2000), and the K^+ channel $K_v4.2$ (Chu et al., 2006), suggesting that KIF17 transports a more restricted set of dendritic proteins that may be segregated early in the secretory pathway. The interaction between KIF17 and NMDA receptors occurs through the GluN2B subunit in an indirect manner via a PDZ protein complex consisting of CASK/mLin2 and Mint1/mLin10 (Setou et al., 2000). Interestingly, CASK associates with NMDA receptors early in the secretory pathway (Jeyifous et al., 2009; Yin et al., 2012), suggesting that KIF17 may direct post-ER transport of receptors. Moreover, the association between KIF17 and Mint1 is itself regulated by CaMKII-dependent phosphorylation (Guillaud et al., 2008). Phosphorylation-dependent uncoupling of KIF17 from Mint1 allows kinesin-cargo

Europe PMC Funders Author Manuscripts

Europe PMC Funders Author Manuscripts

release (Guillaud et al., 2008), suggesting a molecular basis for controlling cargo transport and delivery. Despite their well-documented role in regulating synapse function (Wong et al., 2002; Yin et al., 2011, 2012), it is unclear where along the secretory pathway kinesins direct cargo transport, whether such transport determines local versus long-range trafficking in dendrites, and how the length scale of new cargo delivery is regulated by local synaptic signaling.

Here, we demonstrate that synaptic activity restricts cargo transport between post-ER compartments distributed throughout dendrites. Using a combination of live-cell imaging and fluorescent reporters of transport through the secretory pathway, we show that tubulovesicular carriers emerge from ER exit sites in dendrites in close association with ERGIC and Golgi outposts (GOs). In the absence of synaptic activity, post-ER carriers undergo long-range transport that explores dendritic lengths over tens of microns. In contrast, elevated synaptic activity spatially confines post-ER trafficking and accelerates the accumulation of new secretory cargo at the plasma membrane. In turn, this activity-dependent confinement requires Ca^{2+}/calmodulin-dependent protein kinase (CaMK) activity and phosphorylation of KIF17 at a specific CaMK type II (CaMKII) site. Together, our results indicate that postsynaptic activity confines and spatially focuses early secretory trafficking by KIF17 phosphorylation, revealing a mechanism for tuning the length scales of new cargo delivery to the dendritic membrane. Activity-dependent control of microtubule-based transport may provide a general paradigm for directing new membrane macromolecules to maintain and modify neuronal function.

Results

Nascent Secretory Cargo Is Processed through ERGIC Clusters throughout Neuronal Dendrites

To monitor secretory trafficking in hippocampal neurons, we imaged the ts045 temperature-sensitive mutant of the vesicular stomatitis virus glycoprotein (VSVG-ts045, hereafter referred to as VSVG), a well-studied secretory cargo (Presley et al., 1997; Toomre et al., 1999). After synthesis and accumulation in the ER at 40°C, a temperature at which VSVG is unable to exit the ER, GFP-tagged VSVG (VSVG-GFP) or mCherry-tagged VSVG (VSVG-mCh) was released and accumulated in post-ER compartments by switching the temperature to 20°C (Griffiths et al., 1985; Matlin and Simons, 1983; Figure 1A). After 3 hr at 20°C, a time period sufficient for complete export from the ER (Horton and Ehlers, 2003; Horton et al., 2005), we assessed VSVG dynamics at physiological temperature. After it was released from the ER, VSVG accumulated in discrete structures distributed throughout dendrites, especially at branch points, which remained at the same position for seconds to minutes (Figure 1B). In addition, post-ER cargo was present in smaller tubulovesicular carriers that were much more dynamic and moved in both retrograde and anterograde directions (Figure 1B; Movie S1). In many instances, tubulovesicular carriers merged with and formed from these stationary post-ER compartments (Figure 1B; Movies S1 and S2), indicating that they represent sites of cargo exchange. Importantly, Golgi-Snare 27-mCherry (GS27-mCh), an mCherry-tagged version of a naturally occurring protein of the secretory pathway (Lowe et al., 1997), displayed dynamics very similar to that of VSVG (Movie S3).

In contrast to GOs, which are present in only a subset of dendrites (Gardiol et al., 1999; Horton et al., 2005), the observed stationary post-ER organelles are present in all dendrites (Figures 1B, 1D, 2E, and 4B). These structures are smaller than GOs but are morphologically similar to the ERGIC as visualized by ERGIC53 and Rab1B immunolabeling (Figure 1C). Indeed, after a 40°C to 20°C shift, VSVG-mCh showed extensive colocalization with the ERGIC marker GFP-ERGIC53 (Figure 1D). Thus, nascent secretory cargo accumulates in and is transported between clustered ERGICs distributed throughout dendrites. This indicates that, unlike GOs that are largely restricted to primary and proximal dendrites, a distributed collection of ERGICs traffic newly synthesized membrane proteins throughout the dendritic arbor.

Synaptic Activity Spatially Restricts Post-ER Trafficking in Dendrites

Although normally the method of choice, single-particle tracking (SPT) is not well suited to characterize the motion of post-ER carriers due to their irregular shapes and their frequent fusion and fission. We thus developed an alternative method. In brief, we used a two-frame running-subtraction approach, in which the subtracted signal corresponds to moving structures (Hanus et al., 2004; Toomre et al., 1999), to derive a mobility index that captures the global dynamics of tubulovesicular structures (see Experimental Procedures for details). To validate this approach, we first analyzed the movement of latex beads diffusing in media of increasing viscosities, using both our running-subtraction method and SPT (Figure S1A). In this analysis, the bead mobility index was compared with the bead velocity determined by SPT. As predicted by the Stokes-Einstein relation, the bead mobility index decreased exponentially with increasing viscosity (Figure S1B). We found an excellent correlation between the average bead velocity derived from SPT and our global mobility index (Figure S1C), confirming that this two-frame running-subtraction method accurately and quantitatively assesses particle motion.

To determine the effect of neuronal activity on membrane cargo exchange between secretory outposts, we compared the dynamics of post-ER secretory carriers upon pharmacological manipulation of synaptic transmission. We increased synaptic activity by incubating neurons in 4-aminopyridine (4AP, 50 μM), a voltage-gated K^+ channel blocker to increase neuronal firing, and bicuculline (bic, 20 μM) to concomitantly reduce inhibitory transmission in these mixed cultures. Conversely, we decreased excitatory synaptic activity by blocking AMPA- and NMDA-type glutamate receptors with CNQX (50 μM) and AP5 (50 μM), respectively. Post-ER trafficking in dendrites was monitored in young (12–13 days in vitro [DIV]) and older neurons (18–20 DIV), which were sequentially recorded under basal conditions, 15–25 min after the addition of 4AP/bic, and then again 15–25 min after the addition of CNQX/AP5. In both young and older neurons, increasing synaptic activity decreased the mobility of post-ER vesicular trafficking over a period of minutes (Figures 2A and 2B). Conversely, blocking excitatory transmission increased the mobility and spatial range of post-ER trafficking (Figures 2A and 2B). Whereas 4AP/bic had a stronger effect in young neurons, CNQX/AP5 had a strong effect in both young and older cells (Figure 2B), likely indicating a developmental reduction of post-ER trafficking commensurate with the proliferation of synapses and the acquisition of network activity (Jan and Jan, 2003; Verderio et al., 1999). In 18–20 DIV neurons, activity blockade increased vesicular dynamics (Figure 2C),

Europe PMC Funders Author Manuscripts

consistent with a tonic-activity-dependent inhibition of early secretory trafficking. In addition, we compared post-ER trafficking in distinct neurons monitored under basal conditions, in the presence of 4AP/bic, or in the presence of 4AP/bic/CNQX/AP5 (Figure 2D). This population analysis confirmed the results seen after sequential treatment of individual cells (compare Figures 2B and 2D).

In further experiments, we monitored the effect of glutamate receptor blockers after a 30 min exposure to 10 μM glutamate plus 5 μM glycine, a treatment that almost completely arrests post-ER carrier movement (Figure 2E). We found that CNQX plus AP5 restored post-ER trafficking over a period of minutes as indicated by the appearance of dynamic tubulovesicular intermediates shuttling between stable secretory organelles (Figure 2E; Movie S4). Thus, spatial arrest of post-ER transport trafficking is quickly reinstated in the absence of activity. To test whether the activity-induced reduction of lateral vesicular trafficking reflects a global impairment of secretory trafficking, we monitored the accumulation of post-Golgi cargo at the plasma membrane under similar conditions using VSVG-GFP. Immunolabeling of surface VSVG at 0, 60, and 120 min after switching from 40°C to the fully permissive 32°C showed that synaptic activity actually accelerates cargo accumulation at the cell surface (Figure 2F). Thus, reduced mobility of post-ER transport under high activity conditions is not associated with a blockade of cargo delivery to the dendritic plasma membrane. We conclude that neuronal activity induces a spatially confined, direct, and more rapid delivery of new secretory cargo to the dendritic membrane.

To examine the temporal relationship between neuronal activity and post-ER carrier dynamics, we performed dual imaging of secretory trafficking and Ca^{2+} signaling in neurons coexpressing VSVG-tdTomato (VSVG-tdT) and GCaMP3. Neuronal activity in the form of presumptive action potential bursts was revealed by transient increases in GCaMP fluorescence (Tian et al., 2009). Such transient bouts occurred spontaneously (Figure 3A) and could be elicited by field stimulation (Figure 3B). In response to both spontaneous and evoked Ca^{2+} transients, secretory carriers frequently stopped, initiated movement, or changed direction during or immediately after individual Ca^{2+} bursts (Figures 3A and 3B). This tight temporal relationship between Ca^{2+} transients and post-ER carrier mobility provides strong evidence that neuronal activity controls microtubule-dependent transport on a short timescale.

Activity Limits Long-Range Secretory Transport by Phosphorylation of KIF17

The transport of vesicular cargo depends on selective association with microtubule-based motors (Hirokawa et al., 2010; Schlager and Hoogenraad, 2009) whose activity and cargo association are regulated by diverse cellular signals (Guillaud et al., 2008; Hirokawa et al., 2010; Johansson et al., 2007; Macaskill et al., 2009; Niwa et al., 2008). Among microtubule motors, KIF17 regulates the trafficking of select dendritic cargo, and phosphorylation of KIF17 by CaMKII on serine 1029 abrogates binding to the NMDA receptor/CASK/Mint1 complex (Guillaud et al., 2008). We thus hypothesized that neuronal activity might exert a general effect on microtubule-based post-ER transport by phosphorylation of KIF17 through a Ca^{2+} and CaMKII pathway. To test this hypothesis, we compared the dynamics of VSVG-mCh in neurons coexpressing wild-type YFP-tagged KIF17 (KIF17-WT) or a KIF17

S1029A mutant that cannot be phosphorylated by CaMKII (KIF17-S1029A; Figure 4A). Whereas increased neuronal activity (4AP/bic) reduced post-ER trafficking in neurons expressing KIF17-WT, expression of KIF17-S1029A blocked the activity-induced confinement of post-ER trafficking (Figures 4B and 4C; Movie S5). Consistent with a requirement for CaMK activity, the CaMK inhibitor KN93 (10 μM) prevented the reduction of post-ER carrier mobility triggered by 4AP/bic (Figure 4C). This result was confirmed by a phenotypic analysis in which blind observers assessed whether tubulovesicular dynamics were reduced after elevation of synaptic activity (Figures 4D, 4E, and S3). To test for potential CaMK-independent effects of KN93, we used a similar assay to compare KN93 (3.3 μM) with its inactive analog, KN92 (3.3 μM). These experiments were performed in neurons expressing VSVGt-mCh that were imaged directly after release of the ER-exit blockade (no Golgi block; see Experimental Procedures) or after blockade and release of Golgi exit (with Golgi block), and in neurons expressing GS27-mCh. KN92 partially prevented the activity-dependent reduction of secretory trafficking, likely due to the inhibitory effect of KN92 and KN93 on L-type voltage-gated Ca^{2+}channels (Gao et al., 2006). Notably, although KN93 had only a mild effect on post-ER VSVG imaged without a Golgi block (i.e., at early stages of secretory trafficking), it strongly reduced the response of both VSVG after blockade and release of Golgi exit (as in Figure 4B) and GS27 (Figures 4D, 4E, and S2), revealing a selective effect on carriers at later stages of secretory trafficking. Taken together, these results indicate that activity-dependent signaling through a CaMK/KIF17 pathway restricts ERGIC secretory dynamics in dendrites.

Discussion

In the present study, we found that following ER export, nascent secretory cargo accumulates in and traffics through ERGICs distributed throughout neuronal dendrites. During development and upon acute increases in synaptic activity, microtubule-based transport and cargo exchange between these secretory outposts are spatially restricted without preventing cargo exocytosis. This activity-induced spatial confinement of secretory cargo is occluded by site-specific mutations of the kinesin motor KIF17 that prevent phosphorylation by CaMKII. These results define a mechanism for compartmentalized trafficking in dendrites and indicate that synaptic activity can control cargo itinerary through the early secretory pathway.

KIF17 is a direct target for phosphorylation by CaMKII at serine 1029, and this phosphorylation releases KIF17 bound cargo such as GluN2B-containing NMDA receptors (Guillaud et al., 2008). Here, we have shown that activity-dependent disruption of KIF17-cargo interactions prevents long-range transport of post-ER secretory cargo. This is notable because nearly all functions described to date for KIF17 have been attributed to later-stage trafficking of select post-Golgi cargo (Yin et al., 2012), and suggests that tight regulation of kinesin-cargo interactions occurs early in the secretory pathway to define the spatial span of cargo delivery. Interestingly, synaptic activity has opposite effects on kinesins and unconventional class V myosins, and either disrupts (Guillaud et al., 2008; Macaskill et al., 2009) or favors (Correia et al., 2008; Wang et al., 2008) interaction with cognate cargo, respectively. This supports the general notion that neuronal activity promotes highly local cargo transport by both uncoupling cargo from long-range microtubule motors and

Europe PMC Funders Author Manuscripts

Europe PMC Funders Author Manuscripts

promoting association with membrane-proximal, unconventional myosins. Reminiscent of melanophores in which microtubule and actin-based motors are coregulated within multifunctional protein complexes (Kashina et al., 2004), this model suggests that synaptic activity favors cargo unbinding from microtubules and transfer to F-actin for local delivery to exocytic sites at the dendritic plasma membrane.

We previously showed that membrane protein lateral mobility in the ER is regulated by specific synaptic receptors (Cui-Wang et al., 2012).Whereas group I metabotropic glutamate receptors decrease the spatial range of cargo mobility within the ER proper, ionotropic glutamate receptors have a strong impact on post-ER vesicular trafficking (Figure 3) but little effect on cargo dynamics in the ER (Cui-Wang et al., 2012). Thus, distinct glutamatergic synaptic signaling pathways control specific aspects of membrane cargo synthesis and secretory trafficking in dendrites, each contributing to local membrane protein processing.

In PC12 cells, Rab1-containing ERGICs and ER exit sites, but not Golgi membranes, are selectively distributed to the neurites and growth cones of polarized cells (Sannerud et al., 2006), indicating that satellite secretory systems devoid of classical Golgi membranes are formed during neuritogenesis. Our results show that the long-range transport of post-ER cargo becomes progressively limited during neuronal maturation, consistent with the emergence of increasing synaptic activity (Figures 2A–2C). These findings raise the possibility that ion channels and secreted proteins produced in segments of dendrites devoid of Golgi membranes may bypass this compartment (Jeyifous et al., 2009) and use a direct ER-ERGIC-plasma membrane pathway. Given the known impact of Golgi-associated glycosylation on ion channel distribution (Storey et al., 2011), stability (Watanabe et al., 2004), and biophysical properties (Schwetz et al., 2011), it is possible that by bypassing the Golgi, dendritically synthesized neurotransmitter receptors and voltage-gated ion channels may develop more diverse properties, which in turn would impact dendritic excitability.

Local synthesis of secreted factors and membrane proteins contributes to synapse plasticity, and many mRNAs for secreted proteins are themselves transported by kinesin motors (Hirokawa, 2006; Kiebler and Bassell, 2006). Our results implicate KIF17 phosphorylation in local secretory trafficking associated with newly synthesized cargo. The confinement of secretory trafficking reported here may help explain how local synaptic signals direct newly made receptors and secreted proteins to specific dendritic domains. More broadly, such a mechanism may provide a general paradigm for directed cargo delivery in geometrically complex cells.

Experimental Procedures

Cell Culture and Transfection

Neuronal cultures were prepared and transfected as previously described (Cui-Wang et al., 2012; Sutton et al., 2006). Experiments were performed 12–24 hr post transfection in neurons displaying moderate levels of exogenous protein expression. All animal procedures were performed under protocols compliant and approved by the Institutional Animal Care

Europe PMC Funders Author Manuscripts

and Use Committees of Duke University, the Max Planck Society, the University of Bordeaux, and Pfizer.

Imaging and Drug Treatments

Live-cell imaging was performed at 20°C or 37°C with an inverted spinning-disk confocal microscope. Activity-dependent secretory trafficking was assessed in E4 medium supplemented with 4 mM $CaCl_2$ and 0–0.5 mM $MgCl_2$ for a maximum duration of 90 min.

Antibodies and Immunocytochemistry

Unless otherwise specified, immunocytochemistry was performed as described previously (Cui-Wang et al., 2012; Horton and Ehlers, 2003). For Rab1b immunostaining, cells were permeabilized with 0.2% saponin before fixation.

Two-Frame Running Subtraction

Tubulovesicular structures were isolated by wavelet decomposition (Théry et al., 2005). Segmented images were binarized and used for two-frame running subtraction (Hanus et al., 2004; Toomre et al., 1999). A mobility index was calculated by normalizing subtractive surfaces (i.e., the pixels that correspond to objects movements) by average pixel numbers in the source time-lapse sequences (i.e., the total area of the considered objects).

Categorization of Dendritic Kymographs

Pairs of kymographs (control versus 4AP/bic) were sorted as affected (reduced dynamics, or “yes”), unaffected (no reduction, or “no”), or not suitable for such a determination (nondetermined) by five “blind” observers.

Statistics

Data are presented as means ± SEM unless otherwise indicated.

Supplemental Information

Refer to Web version on PubMed Central for supplementary material.

Acknowledgments

We thank Cécile Charrier and Georgi Tushev for their critical reading of the manuscript. We thank Ina Bartnik, Nicole Fürst, Helene Geptin, Marguerita Klein, and Irina Lebedeva for excellent technical assistance. We thank Jean-Baptiste Sibarita and Victor Racine for the use of MIA. Work in the laboratory of E.M.S. is supported by the Max Planck Society, the European Research Council, DFG CRC 902, and the DFG Cluster of Excellence for Macromolecular Complexes. C.H. is supported by a Marie Curie career integration grant. Work in the laboratory of M.D.E. is supported by Pfizer, Inc., and M.D.E. is an employee and shareholder of Pfizer.

References

Cajigas IJ, Tushev G, Will TJ, tom Dieck S, Fuerst N, Schuman EM. The local transcriptome in the synaptic neuropil revealed by deep sequencing and high-resolution imaging. Neuron. 2012; 74:453–466. [PubMed: 22578497]

Chu PJ, Rivera JF, Arnold DB. A role for Kif17 in transport of Kv4.2. J Biol Chem. 2006; 281:365–373. [PubMed: 16257958]

Correia SS, Bassani S, Brown TC, Lisé MF, Backos DS, El-Husseini A, Passafaro M, Esteban JA. Motor protein-dependent transport of AMPA receptors into spines during long-term potentiation. Nat Neuro-sci. 2008; 11:457–466.

Cui-Wang T, Hanus C, Cui T, Helton T, Bourne J, Watson D, Harris KM, Ehlers MD. Local zones of endoplasmic reticulum complexity confine cargo in neuronal dendrites. Cell. 2012; 148:309–321. [PubMed: 22265418]

Gao L, Blair LA, Marshall J. CaMKII-independent effects of KN93 and its inactive analog KN92: reversible inhibition of L-type calcium channels. Biochem Biophys Res Commun. 2006; 345:1606–1610. [PubMed: 16730662]

Gardiol A, Racca C, Triller A. Dendritic and postsynaptic protein synthetic machinery. J Neurosci. 1999; 19:168–179. [PubMed: 9870948]

Govindarajan A, Israely I, Huang SY, Tonegawa S. The dendritic branch is the preferred integrative unit for protein synthesis-dependent LTP. Neuron. 2011; 69:132–146. [PubMed: 21220104]

Griffiths G, Pfeiffer S, Simons K, Matlin K. Exit of newly synthesized membrane proteins from the trans cisterna of the Golgi complex to the plasma membrane. J Cell Biol. 1985; 101:949–964. [PubMed: 2863275]

Guillaud L, Wong R, Hirokawa N. Disruption of KIF17-Mint1 interaction by CaMKII-dependent phosphorylation: a molecular model of kine-sin-cargo release. Nat Cell Biol. 2008; 10:19–29. [PubMed: 18066053]

Hanus C, Ehlers MD. Secretory outposts for the local processing of membrane cargo in neuronal dendrites. Traffic. 2008; 9:1437–1445. [PubMed: 18532987]

Hanus C, Vannier C, Triller A. Intracellular association of glycine receptor with gephyrin increases its plasma membrane accumulation rate. J Neurosci. 2004; 24:1119–1128. [PubMed: 14762130]

Hirokawa N. mRNA transport in dendrites: RNA granules, motors, and tracks. J Neurosci. 2006; 26:7139–7142. [PubMed: 16822968]

Hirokawa N, Niwa S, Tanaka Y. Molecular motors in neurons: transport mechanisms and roles in brain function, development, and disease. Neuron. 2010; 68:610–638. [PubMed: 21092854]

Horton AC, Ehlers MD. Dual modes of endoplasmic reticulum-to-Golgi transport in dendrites revealed by live-cell imaging. J Neurosci. 2003; 23:6188–6199. [PubMed: 12867502]

Horton AC, Rácz B, Monson EE, Lin AL, Weinberg RJ, Ehlers MD. Polarized secretory trafficking directs cargo for asymmetric dendrite growth and morphogenesis. Neuron. 2005; 48:757–771. [PubMed: 16337914]

Jan YN, Jan LY. The control of dendrite development. Neuron. 2003; 40:229–242. [PubMed: 14556706]

Jeyifous O, Waites CL, Specht CG, Fujisawa S, Schubert M, Lin EI, Marshall J, Aoki C, de Silva T, Montgomery JM, et al. SAP97 and CASK mediate sorting of NMDA receptors through a previously unknown secretory pathway. Nat Neurosci. 2009; 12:1011–1019. [PubMed: 19620977]

Johansson M, Rocha N, Zwart W, Jordens I, Janssen L, Kuijl C, Olkkonen VM, Neefjes J. Activation of endosomal dynein motors by stepwise assembly of Rab7-RILP-p150Glued, ORP1L, and the receptor betalll spectrin. J Cell Biol. 2007; 176:459–471. [PubMed: 17283181]

Kashina AS, Semenova IV, Ivanov PA, Potekhina ES, Zaliapin I, Rodionov VI. Protein kinase A, which regulates intracellular transport, forms complexes with molecular motors on organelles. Curr Biol. 2004; 14:1877–1881. [PubMed: 15498498]

Kayadjanian N, Lee HS, Piña-Crespo J, Heinemann SF. Localization of glutamate receptors to distal dendrites depends on subunit composition and the kinesin motor protein KIF17. Mol Cell Neurosci. 2007; 34:219–230. [PubMed: 17174564]

Kennedy MJ, Ehlers MD. Mechanisms and function of dendritic exocytosis. Neuron. 2011; 69:856–875. [PubMed: 21382547]

Kiebler MA, Bassell GJ. Neuronal RNA granules: movers and makers. Neuron. 2006; 51:685–690. [PubMed: 16982415]

Lowe SL, Peter F, Subramaniam VN, Wong SH, Hong W. A SNARE involved in protein transport through the Golgi apparatus. Nature. 1997; 389:881–884. [PubMed: 9349823]

Macaskill AF, Rinholm JE, Twelvetrees AE, Arancibia-Carcamo IL, Muir J, Fransson A, Aspenstrom P, Attwell D, Kittler JT. Miro1 is a calcium sensor for glutamate receptor-dependent localization of mitochondria at synapses. Neuron. 2009; 61:541–555. [PubMed: 19249275]

Matlin KS, Simons K. Reduced temperature prevents transfer of a membrane glycoprotein to the cell surface but does not prevent terminal glycosylation. Cell. 1983; 34:233–243. [PubMed: 6883510]

Niwa S, Tanaka Y, Hirokawa N. KIF1Bbeta- and KIF1A-mediated axonal transport of presynaptic regulator Rab3 occurs in a GTP-dependent manner through DENN/MADD. Nat Cell Biol. 2008; 10:1269–1279. [PubMed: 18849981]

Presley JF, Cole NB, Schroer TA, Hirschberg K, Zaal KJ, Lippin-cott-Schwartz J. ER-to-Golgi transport visualized in living cells. Nature. 1997; 389:81–85. [PubMed: 9288971]

Sannerud R, Marie M, Nizak C, Dale HA, Pernet-Gallay K, Perez F, Goud B, Saraste J. Rab1 defines a novel pathway connecting the pre-Golgi intermediate compartment with the cell periphery. Mol Biol Cell. 2006; 17:1514–1526. [PubMed: 16421253]

Schlager MA, Hoogenraad CC. Basic mechanisms for recognition and transport of synaptic cargos. Mol Brain. 2009; 2:25. [PubMed: 19653898]

Schwetz TA, Norring SA, Ednie AR, Bennett ES. Sialic acids attached to O-glycans modulate voltage-gated potassium channel gating. J Biol Chem. 2011; 286:4123–4132. [PubMed: 21115483]

Setou M, Nakagawa T, Seog DH, Hirokawa N. Kinesin super-family motor protein KIF17 and mLin-10 in NMDA receptor-containing vesicle transport. Science. 2000; 288:1796–1802. [PubMed: 10846156]

Storey GP, Opitz-Araya X, Barria A. Molecular determinants controlling NMDA receptor synaptic incorporation. J Neurosci. 2011; 31:6311–6316. [PubMed: 21525271]

Südhof TC, Rothman JE. Membrane fusion: grappling with SNARE and SM proteins. Science. 2009; 323:474–477. [PubMed: 19164740]

Sutton MA, Ito HT, Cressy P, Kempf C, Woo JC, Schuman EM. Miniature neurotransmission stabilizes synaptic function via tonic suppression of local dendritic protein synthesis. Cell. 2006; 125:785–799. [PubMed: 16713568]

Théry M, Racine V, Pépin A, Piel M, Chen Y, Sibarita JB, Bornens M. The extracellular matrix guides the orientation of the cell division axis. Nat Cell Biol. 2005; 7:947–953. [PubMed: 16179950]

Tian L, Hires SA, Mao T, Huber D, Chiappe ME, Chalasani SH, Petreanu L, Akerboom J, McKinney SA, Schreiter ER, et al. Imaging neural activity in worms, flies and mice with improved GCaMP calcium indicators. Nat Methods. 2009; 6:875–881. [PubMed: 19898485]

Toomre D, Keller P, White J, Olivo JC, Simons K. Dual-color visualization of trans-Golgi network to plasma membrane traffic along microtubules in living cells. J Cell Sci. 1999; 112:21–33. [PubMed: 9841901]

Verderio C, Coco S, Pravettoni E, Bacci A, Matteoli M. Synaptogenesis in hippocampal cultures. Cell Mol Life Sci. 1999; 55:1448–1462. [PubMed: 10518992]

Wang Z, Edwards JG, Riley N, Provance DW Jr, Karcher R, Li XD, Davison IG, Ikebe M, Mercer JA, Kauer JA, Ehlers MD. Myosin Vb mobilizes recycling endosomes and AMPA receptors for postsynaptic plasticity. Cell. 2008; 135:535–548. [PubMed: 18984164]

Watanabe I, Zhu J, Recio-Pinto E, Thornhill WB. Glycosylation affects the protein stability and cell surface expression of Kv1.4 but Not Kv1.1 potassium channels. A pore region determinant dictates the effect of glycosylation on trafficking. J Biol Chem. 2004; 279:8879–8885. [PubMed: 14688283]

Wong RW, Setou M, Teng J, Takei Y, Hirokawa N. Over-expression of motor protein KIF17 enhances spatial and working memory in transgenic mice. Proc Natl Acad Sci USA. 2002; 99:14500–14505. [PubMed: 12391294]

Yin X, Takei Y, Kido MA, Hirokawa N. Molecular motor KIF17 is fundamental for memory and learning via differential support of synaptic NR2A/2B levels. Neuron. 2011; 70:310–325. [PubMed: 21521616]

Yin X, Feng X, Takei Y, Hirokawa N. Regulation of NMDA receptor transport: a KIF17-cargo binding/releasing underlies synaptic plasticity and memory in vivo. J Neurosci. 2012; 32:5486–5499. [PubMed: 22514311]

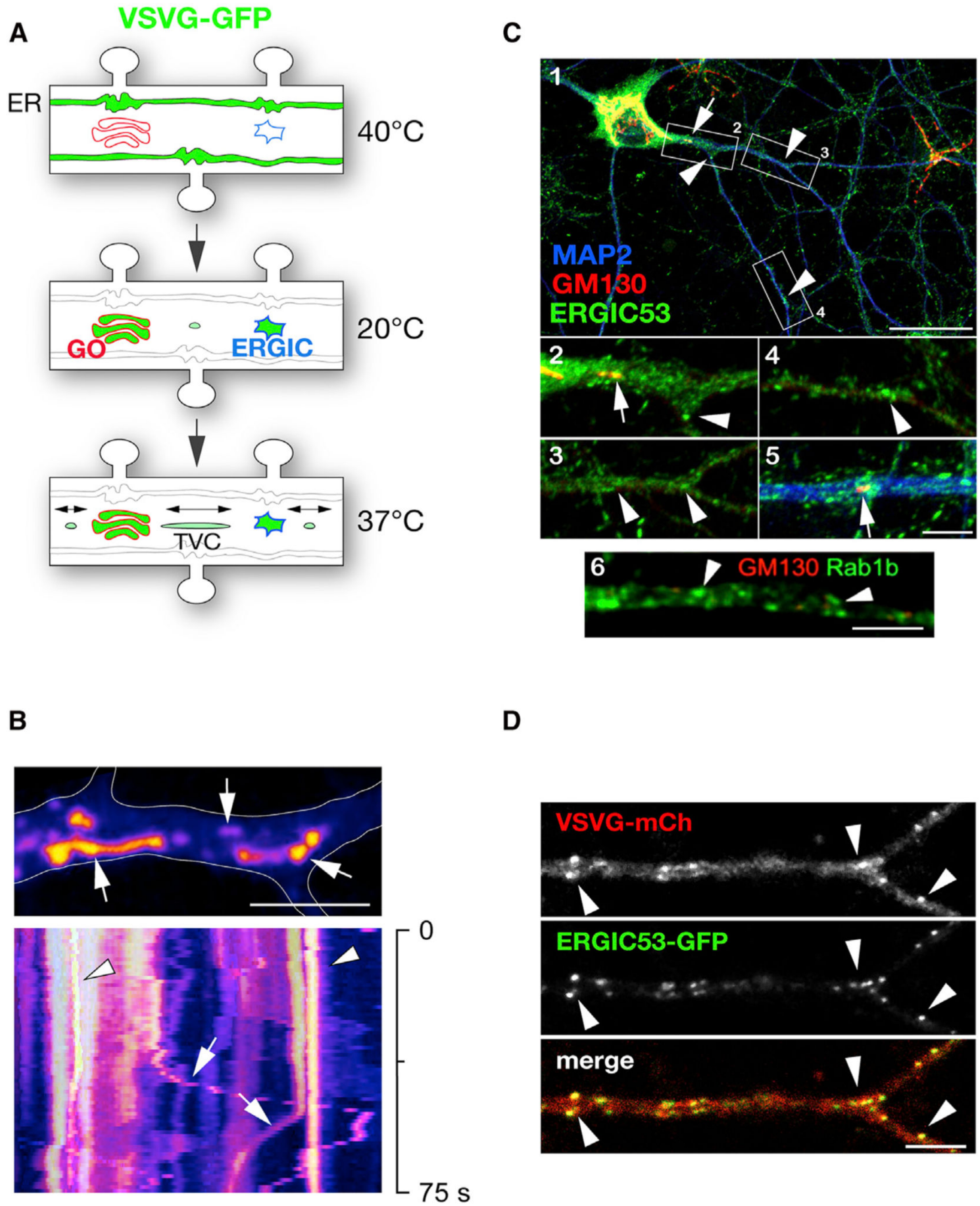

Figure 1. ERGICs Are the Primary Secretory Organelles in Dendrites

(A) Monitoring dendritic secretory trafficking with VSVG-GFP. VSVG-GFP is expressed overnight at 40°C and accumulates in the ER. The temperature is then shifted to 20°C for 3 hr to permit ER exit but prevent post-Golgi trafficking, allowing VSVG to accumulate in post-ER secretory compartments. Post-ER trafficking is then imaged after release from the Golgi by shifting to 37°C. ERGIC, ER-Golgi intermediate compartment; GO, Golgi outpost; TVC, tubulovesicular carrier.

Europe PMC Funders Author Manuscripts

(B) Segregation of early secretory trafficking into stationary compartments and mobile carriers. Top: image of a segment of dendrite (outlined) showing cargo accumulated in post-ER secretory compartments (arrows). Bottom: kymograph (pseudocolored) of VSVG-GFP in the dendrite segment after a switch to 37°C to release the Golgi-exit blockade, showing VSVG trafficking through mobile tubulovesicular carriers (arrows) and stationary post-ER compartments (arrowheads). Scale bar, 5 μm.

(C) Immunolabeling for the *cis*-Golgi matrix protein GM130 (1–6) as a marker of Golgi membranes, ERGIC53 (1–5) and Rab1B (6) as markers of ERGICs, and MAP2 (1 and 5) in segments of dendrites containing (2 and 5) or lacking (3, 4, 6) GOs. Although only a subset of dendrites contain GOs (arrows), all dendrites contain ERGICs (arrowheads). Scale bar, 25 or 5 μm.

(D) VSVG-mCh (red) accumulation in dendritic ERGICs marked with ERGIC53-GFP (green) 42 min after a 40°C to 20°C shift. Scale bar, 5 μm.

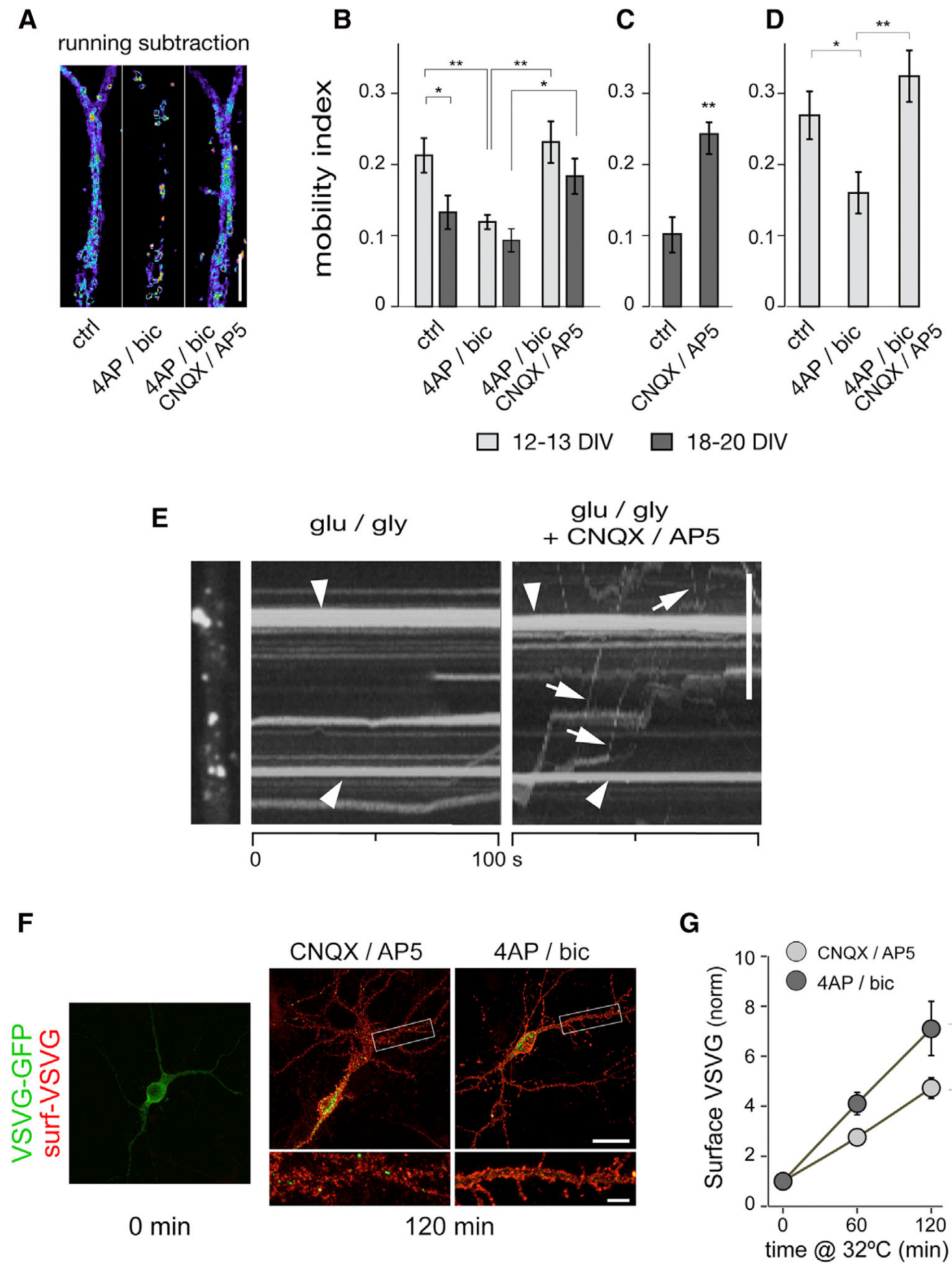

Figure 2. Synaptic Activity Controls Post-ER Secretory Trafficking in Dendrites

(A) Subtractive sequences (projected pseudocolor images) of post-ER dynamics of VSVG-GFP in dendrites recorded under basal conditions 15–25 min after the addition of 50 μM 4-aminopyridine (4AP) plus 20 μM bicuculline (bic), and then again 15–25 min after the addition of 50 μM CNQX plus 50 μM AP5. Scale bar, 5 μm.

(B) Quantification of the mobility index as defined in Figure S1 in young (12–13 DIV) and older (18–20 DIV) hippocampal neurons. n = 16 cells in 2–3 experiments for each group.

Europe PMC Funders Author Manuscripts

(C) Mobility index in individual dendrites of older hippocampal neurons (18–20 DIV) recorded under basal conditions and then 15–25 min after the addition of CNQX/AP5. n = 17 cells in two experiments.

(D) Mobility index in populations of distinct neurons recorded under basal conditions in the presence of 4AP/bic or in the presence of 4AP/bic along with CNQX/AP5. n = 12–14 cells in two experiments.

(E) Shown is a dendrite (image and kymographs) recorded after a 30 min incubation with 10 μM glutamate (glu) plus 5 μM glycine (gly) and then 12 min after the addition of CNQX + AP5. Note the reappearance of mobile tubulovesicular carriers (arrows) shuttling between stationary post-ER compartments upon activity blockade (arrowheads). Scale bar, 5 μm.

(F and G) Images (F) and normalized levels (G) of surface VSVG-GFP (red) at 0, 60, and 120 min after release of ER-exit blockade (40°C to 32°C shift) in the presence of 4AP/bic or CNQX/AP5. Note the increased appearance of surface VSVG in the presence of 4AP/bic. n = 14–25 neurons per condition, 2 experiments. Scale bar, 25 or 5 μm.

*$p < 0.05$, **$p < 0.01$ ANOVA (B, D, and G) and t test (C). Data shown in (B)–(D) and (G) are means ± SEM. See also Figure S1.

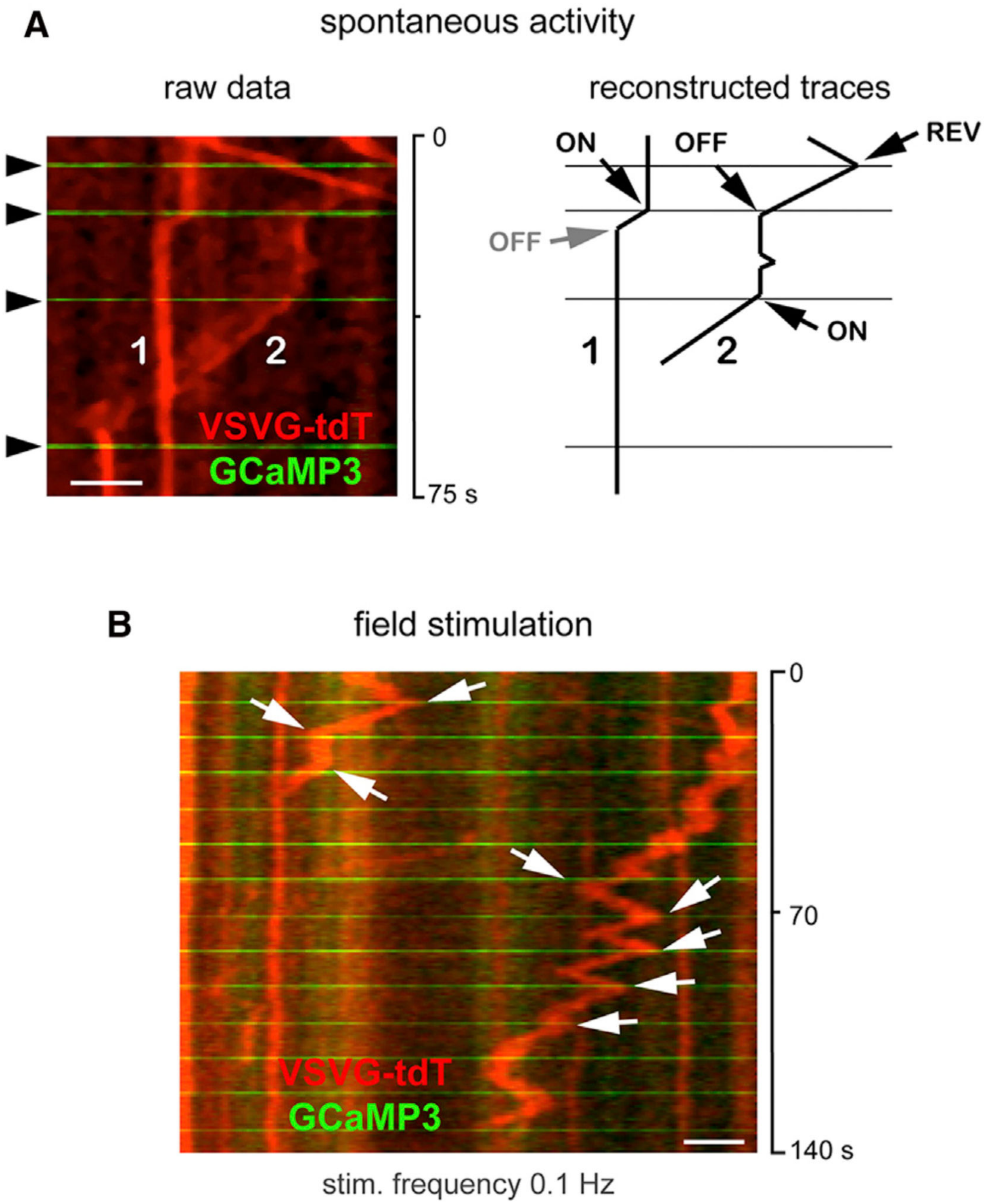

Figure 3. Acute Response of Dendritic Secretory Carriers to Neuronal Activity

(A and B) Kymographs of dendrites expressing VSVG-tdTomato (VSVG-tdT, red) and the Ca^{2+} indicator GCaMP3 (green) during spontaneous neuronal activity (A) or electrical stimulation (B). The right panel in (A) shows reconstructed traces of secretory carrier movements and Ca^{2+} bursts. Ca^{2+} bursts are indicated by transient dendrite-wide green fluorescence, which in kymographs appears as horizontal lines marked by arrowheads in the left panel in (A). Note the abrupt changes in the dynamics of individual secretory carriers (arrows) during Ca^{2+} bursts. In (B), field stimulation was delivered at 0.1 Hz. Evoked Ca^{2+}

responses indicated by horizontal green lines occurred with high fidelity in response to field stimulation and were frequently accompanied by starts, stops, and reversals of individual secretory carriers. Scale bar, 5 µm.

Europe PMC Funders Author Manuscripts

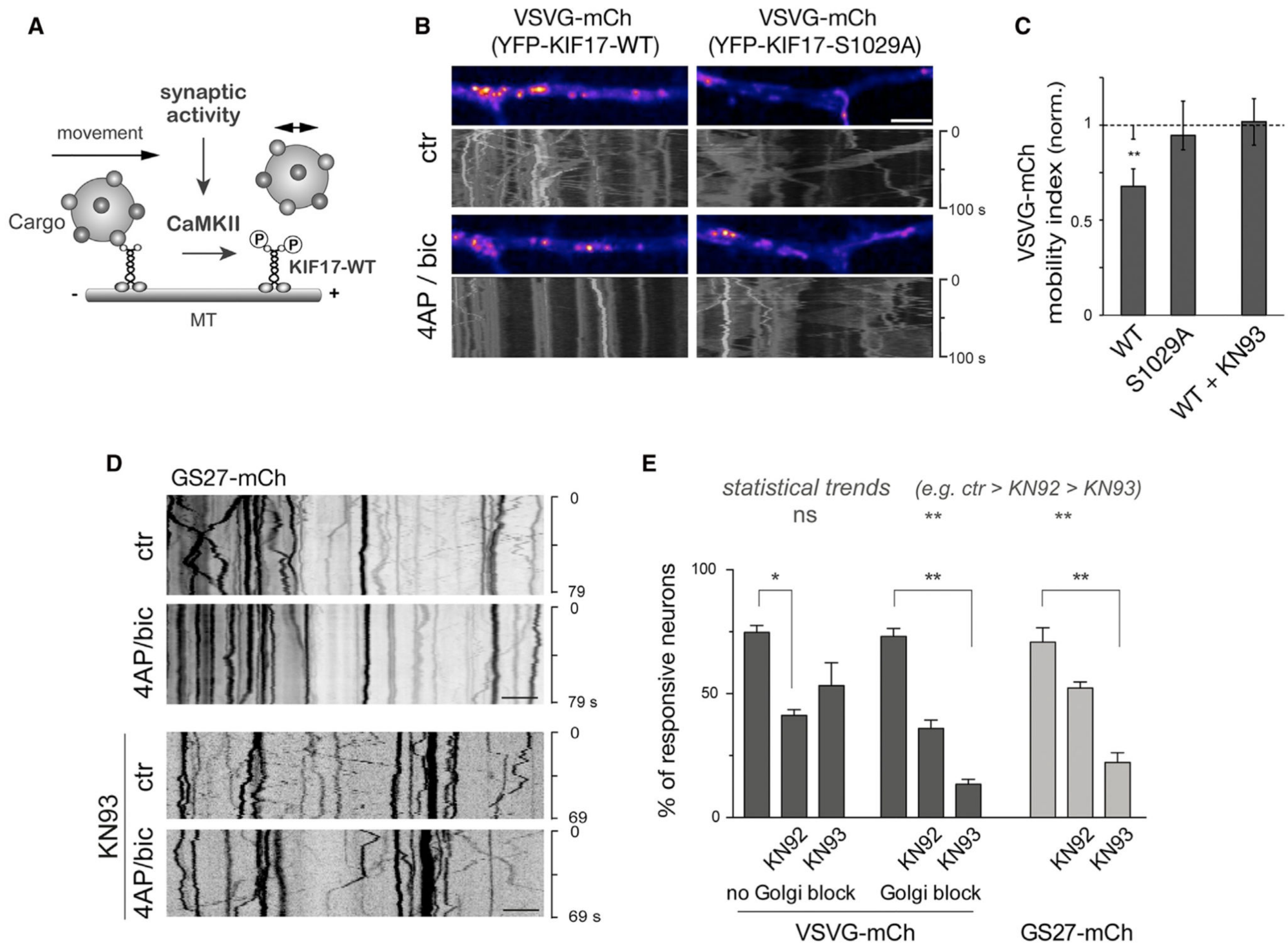

Figure 4. Phosphorylation of KIF17 Mediates Activity-Induced Spatial Confinement of Dendritic Secretory Cargo

(A) Schematic of the effect of synaptic activity on KIF17-dependent transport. Activity-dependent CaMKII phosphorylation of serine 1029 disrupts KIF17 interaction with its cognate cargo and releases cargo-containing vesicles, impairing long-range transport along microtubules. MT, microtubule.

(B) Images (pseudocolor) and kymographs of post-ER VSVG-mCh carriers in neurons expressing KIF17-WT or KIF17-S1029A, before (ctr) or after addition of 4AP plus bicuculline (4AP/bic). Scale bar, 5 μm.

(C) VSVG mobility index in 11—14 DIV neurons expressing YFP-KIF17-WT or YFP-KIF17-S1029A after addition of 4AP/bic in the absence or presence of the CaMK inhibitor KN93 (10 μM). Shown are means ± SEM normalized to control values of untreated neurons. n = 8–15 cells in 1 (KN93), 5 (KIF17-WT), and 4 (KIF17-S1029A) experiments. $^{**}p < 0.01$; t test.

(D) Ca^{2+}/CaMK activity regulates the mobility of Golgi vesicles visualized by GS27-mCh. Kymographs show GS27-mCh movement in neurons before (ctr) or after addition of 4AP/bic in the absence (upper panels) or presence of KN93 (lower panels).

Europe PMC Funders Author Manuscripts

(E) Effect of KN92 and KN93 on the activity-dependent dynamics of VSVG-mCh and GS27-mCh. VSVG-mCh was imaged either directly after release of an ER-exit blockade (no Golgi block) or after blockade and release of Golgi exit(with Golgi block). Shown are percentages of neurons with reduced tubulovesicular dynamics following 4AP/bic (mean ± SEM, n = 4–5 observers; see Experimental Procedures) and statistical trends determined from corresponding cell counts (see also Figure S3). KN92 partially blocked the effect of neuronal activity on secretory dynamics. In contrast, KN93 had a mild effect on post-ER VSVG imaged without a Golgi block, but strongly reduced the mobility of both VSVG imaged after release of a Golgi block and GS27. n = 7–27 cells in 2–8 independent experiments. *$p < 0.05$; **$p < 0.01$; chi-square test for trends (statistical trends) or ANOVA and Dunn's multiple comparison test (bar graph). See also Figures S2 and S3.